

# Secure quantum communication with pseudo-single photon states

Seung-Woo Lee<sup>1</sup> and Jaewan Kim<sup>2</sup>

<sup>1</sup>Quantum Universe Center, Korea Institute for Advanced Study, Seoul 02455, Korea

<sup>2</sup>School of Computational Sciences, Korea Institute for Advanced Study, Seoul 02455, Korea

We introduce an optical quantum state that can fundamentally mimic a single photon state not only with respect to the number of photons but also in terms of an indeterminate phase. Such a state, defined as a state in the superposition of weak coherent states equally distributed on a circle in phase space, is close to a perfect single photon state with almost unit fidelity. Moreover, it exhibits fundamental features of single photons such as Hong-Ou-Mandel interference. Remarkably, by applying it for the implementation of quantum key distribution (QKD), we show that it allows us to achieve higher key generation rates over longer distances than the typical approach using weak coherent states. We expect that our work paves an alternative way to the realization of efficient secure quantum communication as well as photonic quantum information processing.

A single photon is an ideal carrier for quantum communication. Quantum principles such as complementarity and the impossibility of cloning quantum state [1] constitute the fundamental basis of the security of quantum communication [2–6]. Especially, the uncertainty in the measurement of two conjugate variables on single photons is the key feature of quantum key distribution (QKD) protocols [2, 4, 5]. In the realization of quantum communication, single photon sources are thus one of the essential requirements. However, in spite of recent substantial progress [7, 8], a fast and efficient single photon emitter coupled into communication channel (e.g. optical fiber) is still challenging [9].

A strongly attenuated laser, containing less than one photon on average, has been widely accepted as a practical substitute for single photons. Its state can be described by a weak coherent state (WCS) in the form of  $|\sqrt{\mu}e^{i\theta}\rangle = e^{-\mu/2} \sum_{n=0}^{\infty} (\sqrt{\mu}e^{i\theta})^n / \sqrt{n!} |n\rangle$ , where  $\mu$  is the mean photon number,  $\theta$  is the phase of the coherent state, and  $|n\rangle$  is the photon number state. It not only contains more than single photons with a nonzero probability but also distributes uncertainty (roughly) equally between phase and amplitude so that the phase is not indeterminate. The multi-photon issue (e.g. photon-number splitting attack) can be solved with the decoy state method [10, 11]. However, a uniformly random phase - a necessary assumption in this approach [12] - such that, to an eavesdropper without a priori knowledge on the phase, the state is statistically indistinguishable with a Poisson distributed mixed state  $\int_0^{2\pi} |\sqrt{\mu}e^{i\theta}\rangle \langle \sqrt{\mu}e^{i\theta}| d\theta / 2\pi = e^{-\mu} \sum_{n=0}^{\infty} (\mu^n / n!) |n\rangle \langle n|$ , cannot be ideally achieved. An active phase modulator equipped with a random number generator has been commonly used for the phase randomization (except a recent work in [13]). In this direction, the security of QKD with discretized random phase was recently verified [14].

We here introduce an optical quantum state that can fundamentally mimic a single photon state not only with respect to the number of photons but also in terms of an indeterminate phase. This state, which we refer to as *pseudo-single photon state* (PSP), is defined as a super-

position of WCSs equally distributed on a circle in phase space with a perfect discrete random phase. It becomes closer to an ideal single photon state with higher fidelity as the mean photon number decreases or the number of superposed coherent states increases. Remarkably, it exhibits fundamental features of single photons such as the bunching effect with Hong-Ou-Mandel interference. We also note that PSPs can be generated with existing optical technologies e.g. a cross-phase modulation in hollow-core photonic crystal fibers [15, 16]. Finally, by applying PSPs for the implementation of QKD, we demonstrate that higher key generation rates can be achieved over longer distances than the typical approach using WCSs. We expect that our work opens an alternative route to the realization of secure quantum communication and optical quantum information processing.

*Pseudo-number states*- We start with the definition of *pseudo-number states*. In contrast to an ideal photon number state having continuous random phase, we consider discretized phases corresponding to equally distributed coherent states on a circle in phase space,  $\{|\sqrt{\mu}\rangle, |\sqrt{\mu}\omega\rangle, \dots, |\sqrt{\mu}\omega^{d-1}\rangle\}$ . Here,  $\mu$  is the mean photon number of the coherent states and  $\omega = \exp(2\pi i/d)$  with a finite integer  $d$ . We define pseudo-number states as the maximally superposed states of the coherent states

$$|j_d\rangle = \frac{1}{\sqrt{\mathcal{N}_{\mu,j}}} \sum_{q=0}^{d-1} \omega^{-jq} |\sqrt{\mu}\omega^q\rangle \quad (1)$$

where  $j \in \{0, 1, \dots, d-1\}$  and  $\mathcal{N}_{\mu,j}$  is the normalization factor dependent on  $\mu$  and  $j$ , which can be rewritten by  $|j_d\rangle = (d/\sqrt{\mathcal{N}_{\mu,j}}) e^{-\mu/2} \sum_{n \equiv j \pmod{d}}^{\infty} \mu^{n/2} / \sqrt{n!} |n\rangle$ . Conversely, each coherent state on a circle can be represented with the pseudo-number states by  $|\sqrt{\mu}\omega^q\rangle = (1/\sqrt{d}) \sum_{j=0}^{d-1} \omega^{qj} \sqrt{\mathcal{N}_{\mu,j}/d} |j_d\rangle$ .

For large  $\mu$  (in the regime  $\sqrt{\mu} > d$ ),  $|j_d\rangle$  nearly constitute  $d$ -dimensional orthonormal basis [17]. As  $\mathcal{N}_{\mu,j} \rightarrow d$ ,  $|j_d\rangle$  and  $|\sqrt{\mu}\omega^q\rangle$  are in the discrete Fourier transform relations:  $|\sqrt{\mu}\omega^l\rangle = \hat{F}_d |j_d\rangle$  and  $|k_d\rangle = \hat{F}_d^{-1} |\sqrt{\mu}\omega^j\rangle$ , where  $\hat{F}_d = (1/\sqrt{d}) \sum_{k=0}^{d-1} \sum_{l=0}^{d-1} \omega^{kl} |k_d\rangle \langle l_d|$ . On the other hand,

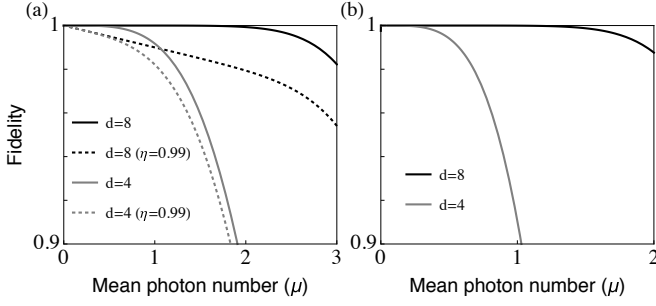


FIG. 1. The fidelities (a) between the ideal single photon  $|1\rangle$  and PSP  $|1_d\rangle$  (solid lines) or PSP under loss  $\eta = 0.99$  (dotted lines) and (b) between the state at the output modes of beam splitter which two PSPs enter different input modes and  $(|2_d\rangle|0_d\rangle - |0_d\rangle|2_d\rangle)/\sqrt{2}$  plotted by changing the mean photon number  $\mu$  for  $d = 4, 8$ .

in the small  $\mu$  regime,  $|j_d\rangle$  can mimic ideal number states, as they become closer to  $|j\rangle$  as  $\mu$  gets smaller or  $d$  increases. The fidelity between  $|j_d\rangle$  and  $|j\rangle$  is given by

$$F(|j\rangle, |j_d\rangle) = |\langle j | j_d \rangle|^2 = \left| \frac{d}{\sqrt{\mathcal{N}_{\mu,j}}} e^{-\mu/2} \frac{\mu^{j/2}}{\sqrt{j!}} \right|^2. \quad (2)$$

In Fig. 1(a), we can see that  $F(|1\rangle, |1_d\rangle)$  approaches to unit as  $\mu$  decreases or  $d$  increases. Remarkably, we can observe the Hong-Ou-Mandel interference with  $|1_d\rangle$ : if two  $|1_d\rangle$  enter different input modes of a beam splitter, the output state of exit modes becomes closer to  $(|2_d\rangle|0_d\rangle - |0_d\rangle|2_d\rangle)/\sqrt{2}$  rapidly as  $\mu$  decreases or  $d$  increases as shown in Fig. 1(b). This is stark contrast to WCSs that cannot exhibit such an interference (details in Appendix). Note that the random mixture of the coherent states  $|\sqrt{\mu}\omega^q\rangle$  can be written in the pseudo-number state representation as

$$\frac{1}{d} \sum_{q=0}^{d-1} |\sqrt{\mu}\omega^q\rangle \langle \sqrt{\mu}\omega^q| = \sum_{j=0}^{d-1} \frac{\mathcal{N}_{\mu,j}}{d^2} |j_d\rangle \langle j_d|, \quad (3)$$

which approaches to the Poisson distributed mixed state as  $d \rightarrow \infty$  (continuous random phase).

The effect of photon losses can be investigated (details in Appendix). We here exclusively consider the loss on  $|1_d\rangle$  with small  $\mu$  for our interest. Under photon losses (with transmission rate  $\eta$ ) [18],  $|1_d\rangle$  is changed into a mixed state  $\rho_d = \{1 - \mu(1 - \eta)\}|1'_d\rangle\langle 1'_d| + \mu(1 - \eta)|0'_d\rangle\langle 0'_d|$ , where  $|1'_d\rangle$  and  $|0'_d\rangle$  are the pseudo-single and -vacuum states with an attenuated amplitude  $\sqrt{\mu\eta}$ . The fidelity  $F(|1\rangle, \rho_d)$  is plotted as dotted lines in Fig. 1(a). It shows that, conditioned on small  $\mu(1 - \eta)$ , PSP under losses still remains being close to the ideal  $|1\rangle$ .

*Generation scheme-* Let us consider a scheme for generating PSPs based on cross-Kerr nonlinearity e.g. in hollow-core photonic crystal fibers, which has been recently realized by experiments in Ref. [15, 16]. Suppose that two-mode coherent states  $|\sqrt{\mu}\rangle_1 |\sqrt{\nu}\rangle_2$  go through a

cross-Kerr medium as illustrated in Fig. 2(a) with the interaction Hamiltonian  $-\hbar\chi\hat{n}_1\hat{n}_2$  for time  $t$ , where  $\hat{n}_i$  is the number operator in  $i$ th mode. We assume that  $\mu$  is small, while  $\nu$  is large enough such that  $\sqrt{\nu} > 2\pi/\chi t$ . Without loss of the generality, if we set  $2\pi/\chi t \equiv d$  as an integer  $\geq 2$ , the state in the output modes can be written by (details in Appendix)

$$e^{\frac{2\pi i}{d}\hat{n}_1\hat{n}_2} |\sqrt{\mu}\rangle_1 |\sqrt{\nu}\rangle_2 \rightarrow \sum_{j=0}^{d-1} \frac{\sqrt{\mathcal{N}_{\mu,j}}}{d} |j_d\rangle_1 |\sqrt{\nu}\omega^j\rangle_2. \quad (4)$$

Therefore, a phase detection in mode 2 (i.e. discrimination of  $j \in \{0, 1, \dots, d-1\}$ ) can identify  $|j_d\rangle$  generated in mode 1. The probability of the generation of each  $|j_d\rangle$  is given by

$$P_{\mu,j} = \frac{\mathcal{N}_{\mu,j}}{d^2} = e^{-\mu} \sum_{n \equiv j \pmod{d}}^{\infty} \frac{\mu^n}{n!}. \quad (5)$$

Note that it becomes the Poisson distribution as  $d \rightarrow \infty$ . With the choice of  $\sqrt{\nu} > d$ , the overlap between the coherent states  $|\sqrt{\nu}\omega^j\rangle$  with different  $j$  on a circle is negligible. In this case, one can consider heterodyne measurements to fully discriminate  $j \in \{0, 1, \dots, d-1\}$ . Alternatively, a scheme to distinguish  $|1_d\rangle$  only from others  $|j(\neq 1)_d\rangle$  can be implemented by using photon on-off detectors as illustrated in Fig. 2 (b). The detection event that only upper detector clicks guarantees that the output state in mode 1 is  $|1_d\rangle$ , which we treat as a triggered event (and others as non-triggered events). The probability of the triggered event is

$$\eta_{\nu,j}^{(t)} = \left| \langle 0 | \sqrt{\eta_{\text{det}}\nu}(\omega^j - \omega) / \sqrt{2} \rangle \right|^2 = \exp[-\eta_{\text{det}}\nu|\omega^j - \omega|^2/4], \quad (6)$$

where  $\eta_{\text{det}}$  is the efficiency of the photon detectors. The dark count at the detector is assumed here to be negligible. The probability of the non-triggered event is then  $\eta_{\nu,j}^{(nt)} = 1 - \eta_{\nu,j}^{(t)}$ . Note that  $\eta_{\nu,1}^{(t)} = 1$  and  $\eta_{\nu,1}^{(nt)} = 0$ . On the other hand,  $\eta_{\nu,j \neq 1}^{(t)}$  tends to decrease as  $\nu$  or  $\eta_a$  increases, while it increases as  $d$  increases. Note that a low

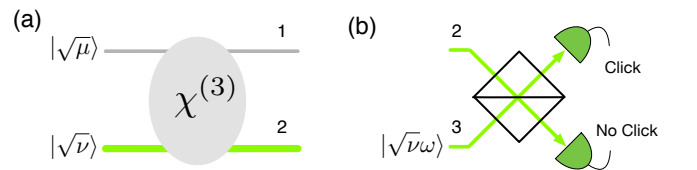


FIG. 2. a. A generation scheme of the pseudo-number states with a cross-Kerr medium. A WCS  $|\sqrt{\mu}\rangle$  enters mode 1, while a strong coherent states  $|\sqrt{\nu}\rangle$  enters mode 2. b. A measurement for the discrimination of PSP from other pseudo-number states. The detection event that only the upper detector clicks (while the lower does not) guarantees the generation of PSP in the output mode 1, which is referred to as a triggered event (otherwise as non-triggered events) in our scheme.

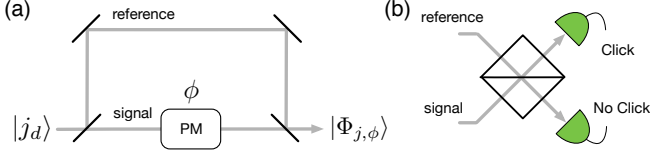


FIG. 3. a. Schematic of the phase encoding QKD scheme on Alice's side. A prepared pseudo-number state  $|j_d\rangle$  is separated into two (one is for signal and the other is for reference) by a 50:50 beam splitter.  $\phi \in \{0, \pi/2, \pi, 3\pi/4\}$  is encoded into the signal with a phase modulator (PM). b. X or Y basis measurement on Bob's side.

detection efficiency  $\eta_{\text{det}}$  can be compensated here with the choice of large  $\nu$ .

*Application to QKD*- We apply PSPs as the source for the implementation of QKD. Suppose that  $|j_d\rangle$  with mean photon number  $2\mu$  is prepared on Alice's side. It enters a phase encoding setup illustrated in Fig. 3(a). The output state is then given by

$$|\Phi_{j,\phi}\rangle = \frac{1}{\sqrt{\mathcal{N}_{2\mu,j}}} \sum_{q=0}^{d-1} \omega^{-jq} |\sqrt{\mu}\omega^q\rangle_r |\sqrt{\mu}\omega^{q+k}\rangle_s, \quad (7)$$

where the subscript  $s(r)$  denotes the signal(reference) state, and  $k = d\phi/2\pi$  denotes the rotated phase in the signal mode for encoding. Note that the randomness of the reference phase is guaranteed by the superposition of the states  $|\sqrt{\mu}\omega^q\rangle$  with  $q \in \{0, \dots, d-1\}$ . This is contrast to the conventional QKD encoding scheme using WCS in the form of  $|\sqrt{\mu}\omega^q\rangle_r |\sqrt{\mu}\omega^{q+k}\rangle_s$ , which requires an additional process for the phase randomization with an active phase modulator and a random number generator [14]. For the Bennett and Brassard 1984 protocol (BB84) [2], logical 0 and 1 are encoded either in X or Y basis, i.e.,  $\{|0_x\rangle_j, |1_x\rangle_j\} = \{|\Phi_{j,0}\rangle, |\Phi_{j,\pi}\rangle\}$  or  $\{|0_y\rangle_j, |1_y\rangle_j\} = \{|\Phi_{j,\pi/2}\rangle, |\Phi_{j,3\pi/4}\rangle\}$ . On Bob's side, a measurement is performed either in X or Y basis as illustrated in Fig. 3(b). For X-basis measurement, the reference and signal states enter the input modes of a beam splitter such that

$$|0_x\rangle_j = \frac{1}{\sqrt{\mathcal{N}_{2\mu,j}}} \sum_{q=0}^{d-1} \omega^{-jq} |\sqrt{\mu}\omega^q\rangle_r |\sqrt{\mu}\omega^q\rangle_s \rightarrow |j_d\rangle|0\rangle$$

$$|1_x\rangle_j = \frac{1}{\sqrt{\mathcal{N}_{2\mu,j}}} \sum_{q=0}^{d-1} \omega^{-jq} |\sqrt{\mu}\omega^q\rangle_r |-\sqrt{\mu}\omega^q\rangle_s \rightarrow |0\rangle|j_d\rangle.$$

Thus, two logical encoding (either 0 and 1) can be discriminated by performing photon on-off detection at the two output modes. Similarly for the Y-basis measurement, two logical encoding can be also discriminated with a modulated beam splitter accordingly.

An essential requirement to guarantee the security of the BB84 protocol is basis indistinguishability, i.e. that Eve cannot distinguish between the logical states encoded

in X and Y basis. It can be investigated by the fidelity  $\mathcal{F}_j(\rho_x, \rho_y)$  between the mixed states of the two encoding,  $\rho_x = |0_x\rangle_j\langle 0_x| + |1_x\rangle_j\langle 1_x|$  and  $\rho_y = |0_y\rangle_j\langle 0_y| + |1_y\rangle_j\langle 1_y|$  (the coefficient is omitted). Following the procedure in Ref. [14], its minimum limit can be obtained as (details in Appendix)

$$\mathcal{F}_j(\rho_x, \rho_y) \geq \frac{d \left| \sum_{q=0}^{d-1} \omega^{jq} e^{-2\mu + \mu\omega^{-q}} (e^{i\mu\omega^{-q}} + ie^{-i\mu\omega^{-q}}) \right|}{\sqrt{2} \mathcal{N}_{2\mu,j}}, \quad (8)$$

which is plotted in Fig. 4 for  $|0_d\rangle$  and  $|1_d\rangle$  by changing  $\mu$  and  $d$ . It shows that the encoded logical states in the two bases are more indistinguishable as  $d$  increases or  $\mu$  gets smaller. From the fact that the encoding of X and Y basis are indistinguishable both in  $|0_d\rangle$  and  $|1_d\rangle$  at small  $\mu$  regime, we can see that a photon loss in PSP is not significantly detrimental to the security of QKD.

*Key generation rate*- We now analyze the key generation rate. For WCSs, the key generation rate can be estimated based on the Gottesman-Lo-Lütkenhaus-Preiskill (GLLP) security analysis as,

$$R \geq -fQ_\mu H(E_\mu) + Q_\mu \Omega \left[ 1 - H(E_\mu/\Omega) \right], \quad (9)$$

where  $Q_\mu$  and  $E_\mu$  are the overall gain and quantum bit error rate (QBER), respectively, for a given mean photon number  $\mu$  of the signal state. Here,  $f$  is the error correction efficiency,  $H(p) = -p \log_2 p - (1-p) \log_2 (1-p)$  is the binary Shannon entropy function, and  $\Omega$  is the fraction of Bob's detection originated from single photon signal emitted from Alice. We take here a pessimistic assumption that all errors are coming from single photon states in the signal. For non-decoy method, the fraction is estimated as  $\Omega = (Q_\mu - P_{\text{multi}})/Q_\mu$ , where  $P_{\text{multi}}$  denotes the probability of Alice's emitting a multi photon state as signal. On the other hand, by using the decoy state method [10, 11], the second term in Eq. (9) is replaced with  $Q_1[1 - H(e_1)]$ , where  $Q_1 = Y_1 \mu e^{-\mu}$  is

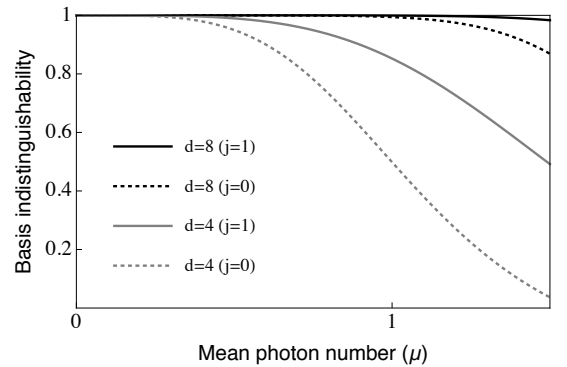


FIG. 4. The basis indistinguishabilities (between X and Y basis) are plotted by changing  $\mu$  for  $d = 4, 8$ . The solid lines denotes the basis indistinguishabilities for  $|1_d\rangle$ , while the dotted lines for  $|0_d\rangle$ .

the gain of the single photon component,  $Y_n$  and  $e_n$  are the yield and QBER for a given photon number  $n$  respectively, and  $\mu e^{-\mu}$  is the probability of generating single photon state in the Poisson distribution. From the underlying assumption of the decoy state method [11], i.e.  $Y_n(\text{decoy}) = Y_n(\text{signal})$  and  $e_n(\text{decoy}) = e_n(\text{signal})$ , Alice can vary  $\mu$  for each signal. The variable  $Y_n$  and  $e_n$  can be deduced with the experimentally measured  $Q_\mu$  and  $E_\mu$ . Therefore, in the decoy state method, Alice can pick up the mean photon number as  $\mu = O(1)$  so that the key rate is obtained as  $O(\eta)$  where  $\eta$  is the overall transmission probability. On the other hand, the optimal  $\mu$  for the non-decoy method is  $\mu = O(\eta)$  yielding the key rate  $R = O(\eta^2)$ . As a result, the decoy method can substantially improve the key generation rate.

Let us then estimate the key generation rate of our scheme. Suppose that Alice prepares a setup for generating  $|j_d\rangle$  with probability  $P_j$  in Eq. (5). The transmission probability of a single photon state is  $\eta = 10^{-0.21L/10}\eta_{Bob}$  with the distance  $L$  and the efficiency of transmission and detection on Bob's side  $\eta_{Bob}$ . The transmission probability for  $n$ -photon signals is  $\eta_n = 1 - (1 - \eta)^n$ . The yield is given by  $Y_n = \eta_n + Y_0 - \eta_n Y_0 = 1 - (1 - Y_0)(1 - \eta)^n$  where  $Y_0$  is the dark count rate. The total gain and QBER are obtained then as  $Q_\mu = Y_0 + \sum_{j=0}^{d-1} \sum_{n \equiv j \pmod{d}}^{\infty} \{1 - (1 - \eta)^n\} e^{-\mu} \mu^n / n! = Y_0 + 1 - e^{-\eta\mu}$  and  $Q_\mu E_\mu = e_0 Y_0 + e_{\text{det}}(1 - e^{-\eta\mu})$ , respectively, where  $e_{\text{det}}$  is the detection error rate. For a non-decoy method, the key generation rate of our scheme can be estimated by Eq. (9) with

$$P_{\text{multi}} = \sum_{j=2}^{d-1} P_{\mu,j} = e^{-\mu} \sum_{j=2}^{d-1} \sum_{n \equiv j \pmod{d}}^{\infty} \frac{\mu^n}{n!}. \quad (10)$$

If  $|j_d\rangle$  is identified with a measurement discriminating  $j$  on Alice's side, we can employ decoy state methods:

i) For the case when  $j$  can be fully identified by e.g. heterodyne measurements with the choice of  $\sqrt{\nu} > d$ , it is possible for Alice and Bob to follow the passive decoy state method [19–21]. One additional thing we should take care of is the fact that pseudo-number states have discrete phases so that the encoding with two bases X and Y are not perfectly indistinguishable. The key generation rate is then estimated as

$$R \geq P_1 Y_1 \left[ 1 - fH(e_1^b) - H(e_1^p) \right], \quad (11)$$

with a pessimistic assumption that all errors occur with  $|1_d\rangle$ . Here,  $\Delta_j = (1 - F_j)/2Y_j$  is defined as basis dependence with the fidelity in Eq. (8), and the bit and phase error rates are given respectively by [12]  $e_j^b = (e_0 - e_{\text{det}})(Y_0/Y_j) + e_{\text{det}}$  and  $e_j^p \leq e_j^b + 4\Delta_j(1 - \Delta_j)(1 - 2e_j^b) + 4(1 - 2\Delta_j)\sqrt{\Delta_j(1 - \Delta_j)}e_j^b(1 - e_j^b)$ .

ii) We then consider the case when only  $|1_d\rangle$  can be discriminated from  $|j(\neq 1)_d\rangle$  e.g. by on-off detectors as illustrated in Fig. 2(b). The gain and QBER for triggered

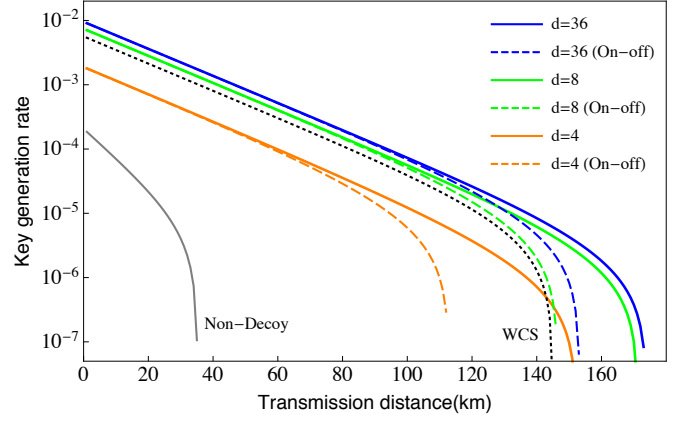


FIG. 5. The key generation rate of the BB84 protocol with PSPs. The solid lines are obtained with a passive decoy state method in the assumption that  $j$  is fully discriminated on Alice side, while the dashed lines are for the case when on-off detectors illustrated in Fig. 2(b) are used. The gray solid line denotes the key rate obtained by a non-decoy method (irrespective of  $d \geq 3$ ). The dotted line is the key rate obtained based on the common approach using WCS and an active decoy state method. For our simulation, the typical experimental parameters in Ref. [22] are used:  $f = 1.16$ ,  $\eta_{\text{det}} = 0.12$ ,  $\eta_{\text{Bob}} = 0.045$ ,  $Y_0 = 1.7 \times 10^{-6}$  and  $e_{\text{det}} = 0.033$ . The mean photon number in the signal is optimized as  $\mu = 1.0, 0.45, 0.08$  for  $d = 36, 8, 4$ , respectively.

and non-triggered events are written by

$$\begin{aligned} Q_\mu^{(t)} &= \sum_{j=0}^{d-1} Q_{\mu,\nu,j}^{(t)}, & E_\mu^{(t)} Q_\mu^{(t)} &= \sum_{j=0}^{d-1} Q_{\mu,\nu,j}^{(t)} e_j, \\ Q_\mu^{(nt)} &= \sum_{j=0}^{d-1} Q_{\mu,\nu,j}^{(nt)}, & E_\mu^{(nt)} Q_\mu^{(nt)} &= \sum_{j=0}^{d-1} Q_{\mu,\nu,j}^{(nt)} e_j. \end{aligned} \quad (12)$$

We define the total ratio  $r \equiv Q_\mu^{(t)}/Q_\mu^{(nt)}$  and the ratio for  $j \neq 1$  as  $r_{\nu,j \neq 1} \equiv Q_{\mu,\nu,j}^{(t)}/Q_{\mu,\nu,j}^{(nt)} = \eta_{\nu,j}/\eta_{\nu,j}^{(nt)}$ , which are experimentally known parameters by Eq. (6). From the fact that  $r_{\nu,2} \geq r_{\nu,j \geq 2}$  and  $r_{\nu,2} = r_{\nu,0}$ , we can see that  $Q_{\mu,\nu,j}^{(t)} \leq r_{\nu,0} Q_{\mu,\nu,j}^{(nt)}$  is always satisfied for  $j \geq 2$ , which can be rewritten by  $Q_\mu^{(t)} - Q_{\mu,\nu,0}^{(t)} - Q_{\mu,\nu,1}^{(t)} \leq r_{\nu,0}(Q_\mu^{(nt)} - Q_{\mu,\nu,0}^{(nt)})$ . Since its left side is equal to  $rQ_\mu^{(nt)} - r_{\nu,0}Q_{\mu,\nu,0}^{(nt)} - Q_{\mu,\nu,1}^{(t)}$ , we arrive at

$$Q_{\mu,\nu,1}^{(t)} \geq (r - r_{\nu,0})Q_\mu^{(nt)}. \quad (13)$$

The maximal QBER is also obtained as

$$\begin{aligned} e_1^b &\leq \frac{E_\mu^{(t)} Q_\mu^{(t)} - e_0 Q_{\mu,\nu,0}^{(t)}}{Q_{\mu,\nu,1}^{(t)}} \\ &= \frac{r E_\mu^{(t)} Q_\mu^{(nt)} - e_0 r_{\nu,0} Q_{\mu,\nu,0}^{(nt)}}{Q_{\mu,\nu,1}^{(t)}} \leq \frac{r E_\mu^{(t)} Q_\mu^{(nt)}}{Q_{\mu,\nu,1}^{(t)}}. \end{aligned} \quad (14)$$

As a result, the key generation rate can be estimated as

$$R \geq -fQ_{\mu}^{(t)}H(E_{\mu}^{(t)}) + \min \left\{ Q_{\mu,\nu,1}^{(t)} \left[ 1 - H(e_1^p) \right] \right\}. \quad (15)$$

The key generation rates obtained by our scheme are plotted in Fig. 5. It shows that QKD implementation with PSPs can substantially increase the key generation rate. It enables to secure QKD at longer distances than a typical approach with WCSs. For example, PSPs with  $d \geq 8$  allow us to obtain higher key generation rate than an active decoy state method using phase randomized WCSs, even with photon detectors with low efficiencies ( $\eta_{\text{det}} = 0.12$ ) as shown in Fig. 5.

*Remarks-* We have introduced an optical quantum state called pseudo-single photon state (PSP) that fundamentally mimics a single photon state. Not only it is close to a perfect single photon state with respect to the fidelity but also it can exhibit fundamental features of single photons such as Hong-Ou-Mandel interference. Remarkably, by applying PSPs for QKD, we demonstrate that higher key generation rates can be achieved over longer distances than a typical QKD scheme with WCSs. Note that our scheme does not necessitate active phase modulation or random number generator, which are possibly a security loophole due to device imperfections.

PSPs can be generated through a cross-phase modulation technique, which has been realized by experiments in various systems [15, 16, 23–28]. They were mostly aimed at implementing quantum non-destructive measurements [29] or two-qubit gate operations [30, 31], which are still demanding due to the requirement of either a strong non-linearity or additional schemes with precise controls [32]. By contrast, a weak nonlinearity even along with source or detector imperfections would suffice to implement our scheme. The cross-phase modulation in photonic crystal fibers demonstrated recently in Ref. [15, 16] may be a suitable candidate, as they have fast response time and can be realized with laser sources at room temperature.

Exploring further applications of PSPs in quantum information processing will be our next step of research. We expect that our work paves an alternative way to the realization of efficient secure quantum communication as well as photonic quantum information processing.

- [7] M. D. Eisaman, J. Fan, A. Migdall, and S. V. Polyakov, *Review of Scientific Instruments* **82**, 071101 (2011).
- [8] I. Aharonovich, D. Englund, and M. Toth, *Nature Photonics* **10**, 631 (2016).
- [9] P.-I. Schneider *et al.* *Optics Express* **26**, 8479 (2018).
- [10] W. Y. Hwang, *Phys. Rev. Lett.* **91**, 057901 (2003).
- [11] H.-K. Lo, X. Ma, and K. Chen, *Phys. Rev. Lett.* **94**, 230504 (2005).
- [12] H.-K. Lo and J. Preskill, *Quantum Inf. Comput.*, **7**, 0431 (2007).
- [13] Z. L. Yuan *et al.*, *Phys. Rev. X* **6**, 031044 (2016).
- [14] Z. Cao, Z. Zhang, H.-K. Lo, and X. Ma, *New J. Phys.* **17**, 053014 (2015).
- [15] N. Matsuda, R. Shimizu, Y. Mitsumori, H. Kosaka, and K. Edamatsu, *Nature Photonics* **3**, 95 (2009).
- [16] V. Venkataraman, K. Saha, and A. L. Gaeta, *Nature Photonics* **7**, 138 (2012).
- [17] J. Kim *et al.* *Optics Communication* **337**, 79 (2015).
- [18] S. J. D. Phoenix, *Phys. Rev. A* **41**, 5132 (1990).
- [19] M. Maurer and C. Silberhorn, *Phys. Rev. A* **75**, 050305(R) (2007).
- [20] Y. Adachi, T. Yamamoto, M. Koashi, and N. Imoto, *Phys. Rev. Lett.* **99**, 180503 (2007).
- [21] X. Ma, and H.-K. Lo, *New J. Phys.* **10**, 073018 (2008).
- [22] C. Gobby, Z. L. Yuan, and A. J. Shields, *Applied Physics Letters* **84** 3762 (2004).
- [23] O. Firstenberg *et al.* *Nature* **502** 71 (2013).
- [24] I.-C. Hoi *et al.* *Phys. Rev. Lett.* **111**, 053601 (2013).
- [25] A. Feizpour, M. Hallaji, G. Dmochowski, and A. M. Steinberg, *Nature Physics* **11** 905 (2015).
- [26] D. Tiarks, S. Schmidt, G. Rempe, and S. Dürr, *Science Advances* **2**, e1600036 (2016).
- [27] K. M. Becka, M. Hosseinia, Y. Duana, and V. Vuletić, *PNAS* **113** 9740 (2016).
- [28] Z.-Y. Liu *et al.* *Phys. Rev. Lett.* **117**, 203601 (2016).
- [29] W. J. Munro, K. Nemoto, R. G. Beausoleil, and T. P. Spiller, *Phys. Rev. A* **71**, 033819 (2005).
- [30] K. Nemoto and W. J. Munro, *Phys. Rev. Lett.* **93**, 250502 (2004).
- [31] W. J. Munro, K. Nemoto, and T. P. Spiller, *New J. Phys.* **7**, 137 (2005).
- [32] H. Jeong, *Phys. Rev. A* **73**, 052320 (2006).

- 
- [1] W. Wootters and W. Zurek, *Nature* **299** 802-803 (1982).
  - [2] C. H. Bennett and G. Brassard, *Proceedings of IEEE International Conference on Computers, Systems, and Signal Processing*, 175-179 (IEEE Press, 1984).
  - [3] A. K. Ekert, *Phys. Rev. Lett.* **67**, 661 (1991).
  - [4] N. Gisin, G. Ribordy, W. Tittel, and H. Zbinden, *Rev. Mod. Phys.* **74**, 145 (2002).
  - [5] V. Scarani *et al.*, *Rev. Mod. Phys.* **81**, 1301 (2002).
  - [6] H.-K. Lo, M. Curry, and K. Tamaki, *Nature Photonics* **8**, 595 (2014).

## Appendix

### HONG-OU-MANDEL INTERFERENCE

Suppose that two PSPs with the same mean photon number  $\mu$  enter different input modes of a 50:50 beam splitter. Then, the state in the two output mode is

$$|1_d\rangle|1_d\rangle \xrightarrow{BS} \frac{1}{\mathcal{N}_{\mu,1}} \sum_{q,q'=0}^{d-1} \omega^{-q-q'} \left| \sqrt{\frac{\mu}{2}}(\omega^q + \omega^{q'}) \right\rangle \left| \sqrt{\frac{\mu}{2}}(\omega^q - \omega^{q'}) \right\rangle. \quad (\text{A1})$$

The fidelity between the state in Eq. (A1) and

$$\frac{1}{\sqrt{2}}(|2_d\rangle|0_d\rangle - |0_d\rangle|2_d\rangle) = \frac{1}{\sqrt{2\mathcal{N}_{\mu,2}\mathcal{N}_{\mu,0}}} \sum_{q,q'=0}^{d-1} (\omega^{-2q} - \omega^{-2q'}) |\sqrt{\mu}\omega^q\rangle |\sqrt{\mu}\omega^{q'}\rangle \quad (\text{A2})$$

can be calculated and plotted by changing the mean photon number  $\mu$  and  $d$ . As presented in the Fig. 1(b) in the main text, we can observe Hong-Ou-Mandel interference with PSPs.

### EFFECTS OF PHOTON LOSSES

Let us consider the effect of photon losses on the pseudo-number states in Eq. (1) in the main text. Their evolution in a lossy environment can be evaluated by solving the master equation [18],

$$\frac{d\rho}{dt} = \gamma(\hat{J} + \hat{L})\rho, \quad (\text{A3})$$

where  $\hat{J}\rho = \sum_i \hat{a}_i \rho \hat{a}_i^\dagger$ ,  $\hat{L}\rho = -\sum_i (\hat{a}_i^\dagger \hat{a}_i \rho + \rho \hat{a}_i^\dagger \hat{a}_i)/2$ . Here,  $\hat{a}_i$  ( $\hat{a}_i^\dagger$ ) is the annihilation (creation) operator for the  $i$ -th mode,  $\gamma$  is the decay constant, and  $\eta = e^{-\gamma t}$  is defined as the transmission rate under loss. The pseudo-number state  $|j_d\rangle$  evolves under losses into

$$\rho_j(t) = \frac{1}{\mathcal{N}_{\mu,j}} \sum_{q,q'=0}^{d-1} \omega^{j(q'-q)} e^{(\omega^{q-q'}-1)\mu(1-\eta)} \times |\sqrt{\mu\eta}\omega^q\rangle \langle \sqrt{\mu\eta}\omega^{q'}|. \quad (\text{A4})$$

For PSP with small  $\mu(1-\eta)$ , it can be written by

$$\begin{aligned} \rho_1(t) &= \frac{1}{\mathcal{N}_{\mu,1}} \sum_{q,q'=0}^{d-1} \omega^{q'-q} e^{(\omega^{q-q'}-1)\mu(1-\eta)} \\ &\quad \times |\sqrt{\mu\eta}\omega^q\rangle \langle \sqrt{\mu\eta}\omega^{q'}| \\ &\approx (1 - \mu(1-\eta)) |1'_d\rangle \langle 1'_d| + \mu(1-\eta) |0'_d\rangle \langle 0'_d| \end{aligned} \quad (\text{A5})$$

where  $|1'_d\rangle$  and  $|0'_d\rangle$  are respectively the pseudo-single and -vacuum states with an attenuated mean photon number  $\mu\eta$ .

### GENERATION OF PSPS WITH CROSS-KERR MEDIUM

The two-mode coherent states  $|\sqrt{\mu}\rangle_1 |\sqrt{\nu}\rangle_2$  go through a cross-Kerr medium with the Hamiltonian  $-\hbar\chi\hat{n}_1\hat{n}_2$  for time  $t$ . We assume that  $\mu$  is small, while  $\nu$  is large enough such that  $\sqrt{\nu} > 2\pi/\chi t$ . Without loss of the generality, we set  $2\pi/\chi t \equiv d$  as an integer  $\geq 2$ . Then, the state in the output modes can be obtained as

$$\begin{aligned} &e^{\frac{2\pi i}{d}\hat{n}_1\hat{n}_2} |\sqrt{\mu}\rangle_1 |\sqrt{\nu}\rangle_2 \\ &= e^{\frac{2\pi i}{d}\hat{n}_1\hat{n}_2} \left( \frac{1}{\sqrt{d}} \sum_{j=0}^{d-1} \sqrt{\frac{\mathcal{N}_{\mu,j}}{d}} |j_d\rangle \right)_1 \left( \frac{1}{\sqrt{d}} \sum_{k=0}^{d-1} |k_d\rangle \right)_2 \\ &= \frac{1}{\sqrt{d}} \sum_{j=0}^{d-1} \sqrt{\frac{\mathcal{N}_{\mu,j}}{d}} |j_d\rangle_1 \left( \frac{1}{\sqrt{d}} \sum_{k=0}^{d-1} \omega^{jk} |k_d\rangle \right)_2 \\ &= \sum_{j=0}^{d-1} \frac{\sqrt{\mathcal{N}_{\mu,j}}}{d} |j_d\rangle_1 |\sqrt{\nu}\omega^j\rangle_2. \end{aligned} \quad (\text{A6})$$

### MINIMUM FIDELITY FOR BASIS INDEPENDENCE

Let us calculate the fidelity between the mixed states of the X and Y basis encoding (the coefficient is omitted),  $\rho_x = |0_x\rangle_j \langle 0_x| + |1_x\rangle_j \langle 1_x|$  and  $\rho_y = |0_y\rangle_j \langle 0_y| + |1_y\rangle_j \langle 1_y|$ , to investigate the basis independence:

$$\begin{aligned} \mathcal{F}_j(\rho_x, \rho_y) &= \mathcal{F}_j \left( |0_x\rangle_j \langle 0_x| + |1_x\rangle_j \langle 1_x|, |0_y\rangle_j \langle 0_y| + |1_y\rangle_j \langle 1_y| \right) \\ &\geq \mathcal{F}_j \left[ |-\rangle |0_x\rangle + |+\rangle |1_x\rangle, |+\rangle |0_y\rangle + |-\rangle |1_y\rangle \right], \end{aligned}$$

which is derived from the fact that the fidelity of two mixed states is the maximum of their purification [14]. By some calculations, we arrive at the minimum fidelity for basis independence,

$$\mathcal{F}_j(\rho_x, \rho_y) \geq \frac{d \left| \sum_{q=0}^{d-1} \omega^{jq} e^{-2\mu+\mu\omega^{-q}} (e^{i\mu\omega^{-q}} + i e^{-i\mu\omega^{-q}}) \right|}{\sqrt{2}\mathcal{N}_{2\mu,j}}. \quad (\text{A7})$$